İSTANBUL UNIVERSITY CERRAHPAŞA

RESEARCH ARTICLE

Electrica, 2021; 21(1): 96-104

A Broadband, Polarization Insensitive, Wide Incidence-Angle-Slotted Ring/Lumped Resistor-Based Metamaterial Absorber for K_u-Band Applications

Sinan Aksimsek

Department of Electrical and Electronics Engineering, Istanbul Kultur University, Istanbul, Turkey

Cite this article as: Aksimsek S. A Broadband, Polarization Insensitive, Wide Incidence-Angle-Slotted Ring/Lumped Resistor-Based Metamaterial Absorber for K_u-Band Applications. *Electrica*, 2021; 21(1): 96-104.

ABSTRACT

A broadband-slotted ring/lumped resistor-based metamaterial absorber (MA) is presented in this study for K_u-band microwave applications. Numerical results of the MA indicate that it can achieve a broadband absorption ratio of more than 85% in the frequency range of 12.4–17.6 GHz and has active polarization insensitivity and wide incidence-angle response over the entire operation band between 12.4-17.6 GHz. The designed MA is ultrathin around λ/14.7 in terms of wavelength at its lowest operation frequency, corresponding to 1.7 mm. The proposed unit-cell structure of the MA is novel, consisting of a slotted ring with eight symmetrically-located lumped resistors, FR-4 material, and a metallic ground, which is compatible with low-cost PCB fabrication; therefore, the MA is suitable for practical microwave applications in the K_u-band.

Keywords: Terms—Broadband, metamaterial absorber, ultrathin, K_u-band

Corresponding Author:
Sinan Aksimsek

E-mail:
s.aksimsek@iku.edu.tr

Received: 08.06.2020

Accepted: 18.08.2020

DOI: 10.5152/electrica.2021.20053

Introduction

Metamaterials are artificial electromagnetic media and have attracted considerable attention over the last decade owing to their unique properties in the subwavelength dimension, such as double negative effect, negative index refraction, and negative permeability, that do not exist in nature Therefore, they are promising for the development of a new class of devices such as perfect lenses [1], antennas [2], imagers [3], absorbers [4, 5], and cloaking platforms [6]. Landy et al. demonstrated the first perfect metamaterial absorber (MA) in 2008. Since then, many MAs providing high efficiency, miniaturization capability, and simple fabrication are proposed, which are not observed in conventional absorber systems such as the Dällenbach layer [7] and Salisbury screen [8]. Typically, MA platforms are formed using different configurations of split rings, enabling the effective tailoring of electric permittivity and magnetic permeability in a narrow or broad bandwidth [9,10]. However, a narrow bandwidth limits their practical applications. Broadband controlling of the constitutive electromagnetic parameters (permittivity and permeability) is key to the development of broadband MAs, which is required for broadband applications over a wide range of the electromagnetic spectrum ranging from microwaves to visible light [10]. In the microwave regime, FR-4 is one of the commonly used and efficient materials for MA fabrication. For instance, Gu et al. presented a unit-cell structure in the form of hexagonal metal-dendritic FR-4, demonstrating a unit-cell absorptivity of 80% within a frequency band of 9.05–11.4 GHz [11]. Moreover, using substrates such as an indium tin oxide film enables the development of optically transparent and broadband radar-wave absorbers [12]. Furthermore, a broadband MA response is achieved with water-based patterns by tuning the height and diameter of water droplets [13]. Various resonance mechanisms, based on different materials and their geometries, have been tested to obtain MAs with a broadband, polarization independence, and wide angle response [14–17]. However, most MA designs focus on the S- and X-bands, and there are few reports on MAs operating in a K_u-band of 12–18 GHz in the microwave regime.

In this study, a broadband MA for K_u-band applications is proposed. Its resonator structure is based on a simple geometry, using a slotted (split) ring with lumped resistors, which is easy

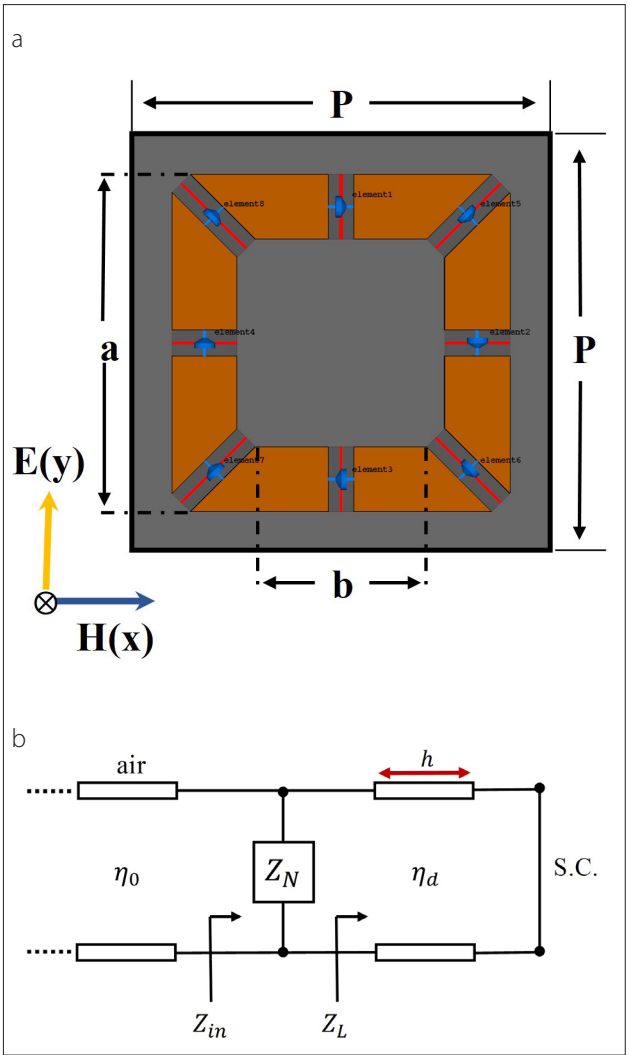

Figure 1. a, b. (a) The top view of the proposed unit cell (b) The transmission line model

to fabricate. Numerical results of the proposed MA prove that it has a broadband, polarization insensitivity, and wide incidence-angle response.

Absorber Design and Principle

The top view of the proposed MA is shown in Figure 1a. The unit cell consists of a slotted ring resonator with eight sections, a dielectric spacer, and a metallic ground. Each metallic section on the top layer is identical, and the metallic pattern is loaded with eight lumped resistors. Copper, which has a conductivity of 5.96×10^7 S/m, is chosen as the metal for the top and bottom layers. The thickness (t) of the top and bottom layers is 0.0035 mm. The dielectric spacer is composed of FR-4, which has a dielectric constant of 4.3 and a loss tangent tans = 0.025. The transmission line model with equivalent lumped parameters is illustrated in Figure 1b. The eight sections with the lumped resistors on the top of the unit cell can be modeled using an RLC circuit network with the equivalent impedance of $Z_N = R + jwL + 1/jwC$. R represents the equivalent resistance of the top metal loaded using the lumped resistors. L and C represent the equivalent inductance and capacitance of the copper layers, respectively. ω is the angular frequency. Z_{in} is the impedance at the input terminals of the metamaterial, which is given as

$$Z_{in} = \frac{Z_N Z_L}{Z_N + Z_L} \tag{1}$$

where Z_L is the load impedance of the short-circuited dielectric spacer, which is expressed as

$$Z_L = j\eta_d \tan(k_d h) \tag{2}$$

where $k_d = \frac{k_0}{\sqrt{\varepsilon_r \mu_r}}$, and ε_r and μ_r are the wavenumber, complex relative permittivity, and permeability of the dielectric substrate. The corresponding reflection coefficient is expressed as

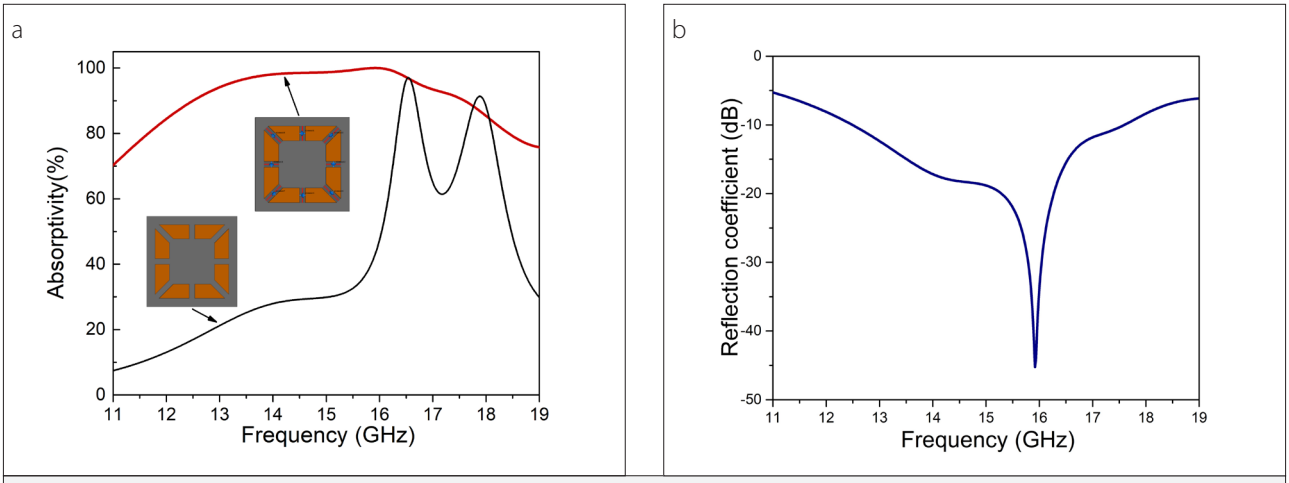

Figure 2. a, b. (a) Absorption spectra of the proposed MA with and without the lumped resistors (b) The reflection coefficient response of the MA with respect the frequency

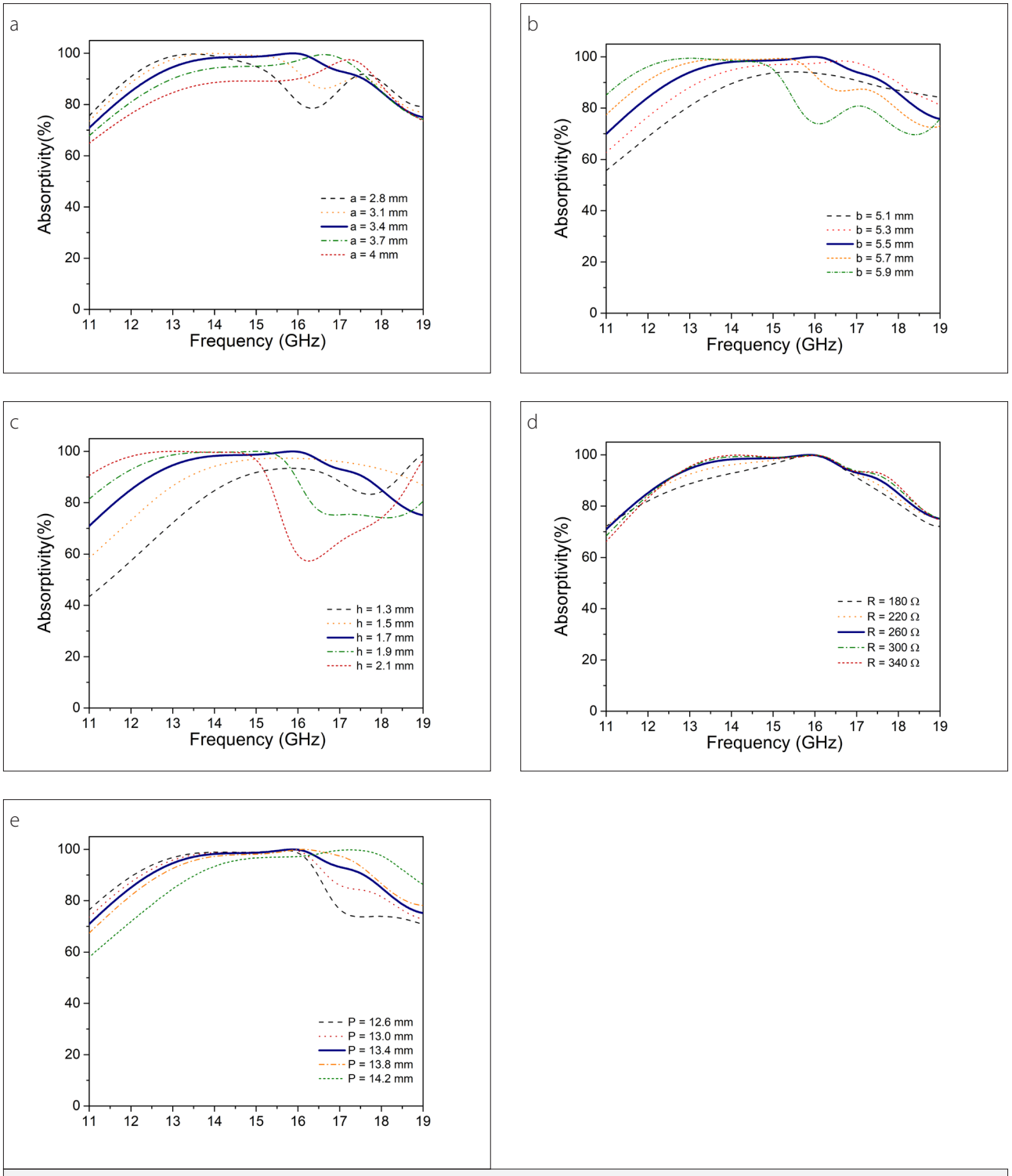

Figure 3. a-e. Absorption spectra of the proposed MA for (a) metallic pattern dimension a (b) metallic pattern dimension b (c) dielectric thickness h (d) lumped resistor R (e) the unit cell dimension P

$$\Gamma = \frac{Z_{in} - Z_0}{Z_{in} + Z_0} \quad (3)$$

where the air impedance $Z_0 = \eta_0 (120\pi\Omega)$. The bottom ground layer blocks signal transmission; hence, the transmission coefficient (T) is zero. When the impedance matching condition

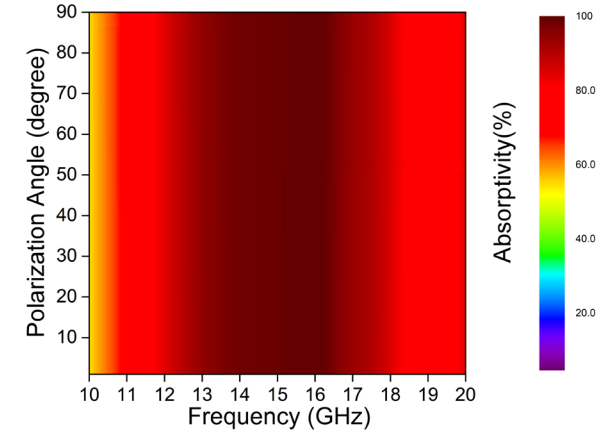

Figure 4. Absorption spectra of the MM as a function of polarization angle (φ) under normal incidence for TE and TM polarizations

between air and the metamaterial is satisfied, Γ will be zero according to Equation (3), leading to unity absorptivity based on the following expression:

$$A = 1 - |\Gamma|^2 - |T|^2 \rightarrow 1 \quad (4)$$

ε_r nd μ of the metamaterial can be tuned by tailoring the size of the unit cell such that $Zin \rightarrow Z_0$, which is the required condition for perfect absorption over the operation frequency band. In this study, the spectral response of the proposed MA was optimized by changing h, the dimensions of the metallic pattern (a and b), and resistance R between the metallic sections. The electromagnetic characterization was performed using a 3D full-wave electromagnetic solver, CST Microwave Studio 2020 (Darmstadt, Germany) based on the finite integration technique (FIT) [18]. The periodic boundary conditions with Floquet ports were used in the x–y plane and the open condition was defined in the z-direction.

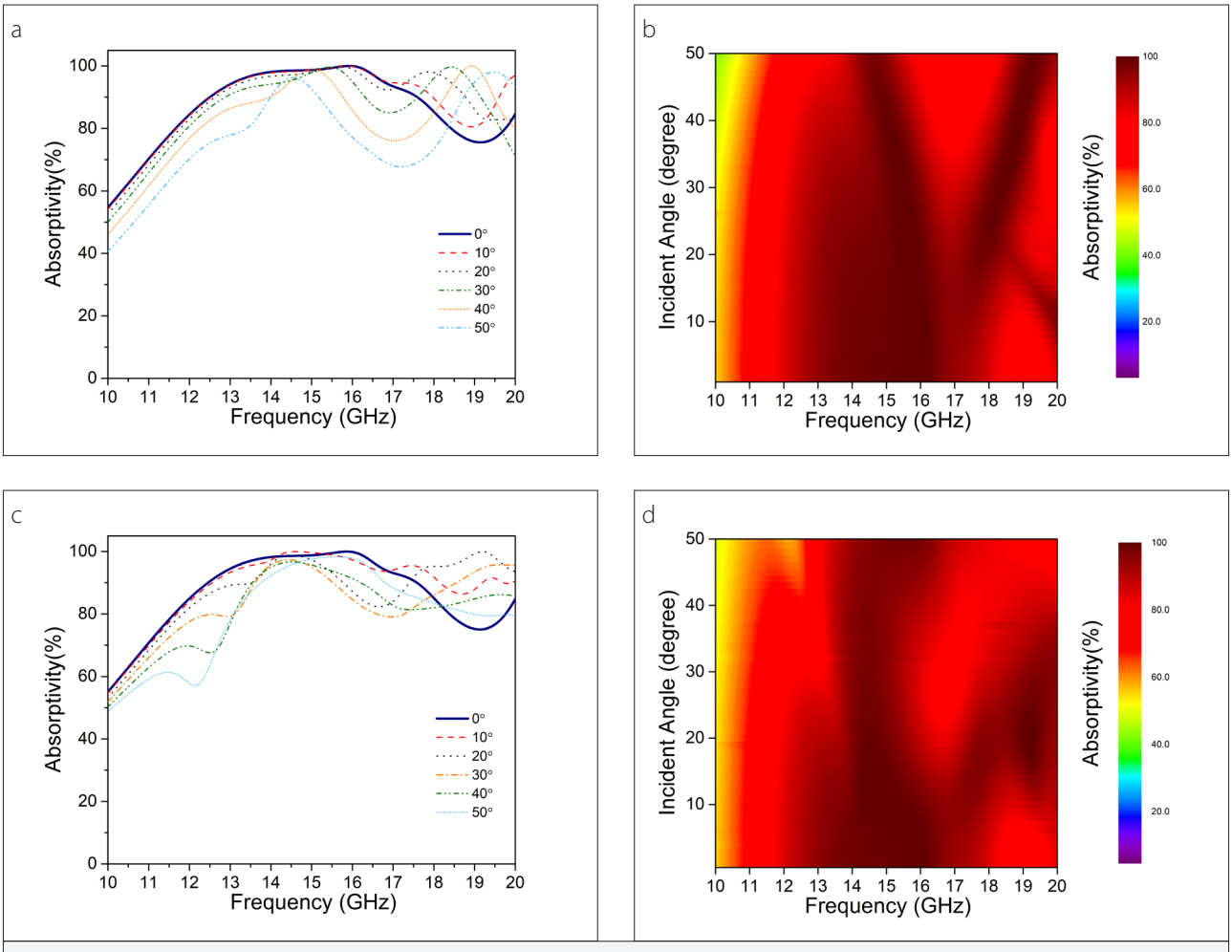

Figure 5. a-d. Absorption spectra of the MM as a function of incident angle for (a) TE polarization (b) TE polarization heatmap (c) TM polarization (d) TM polarization heatmap

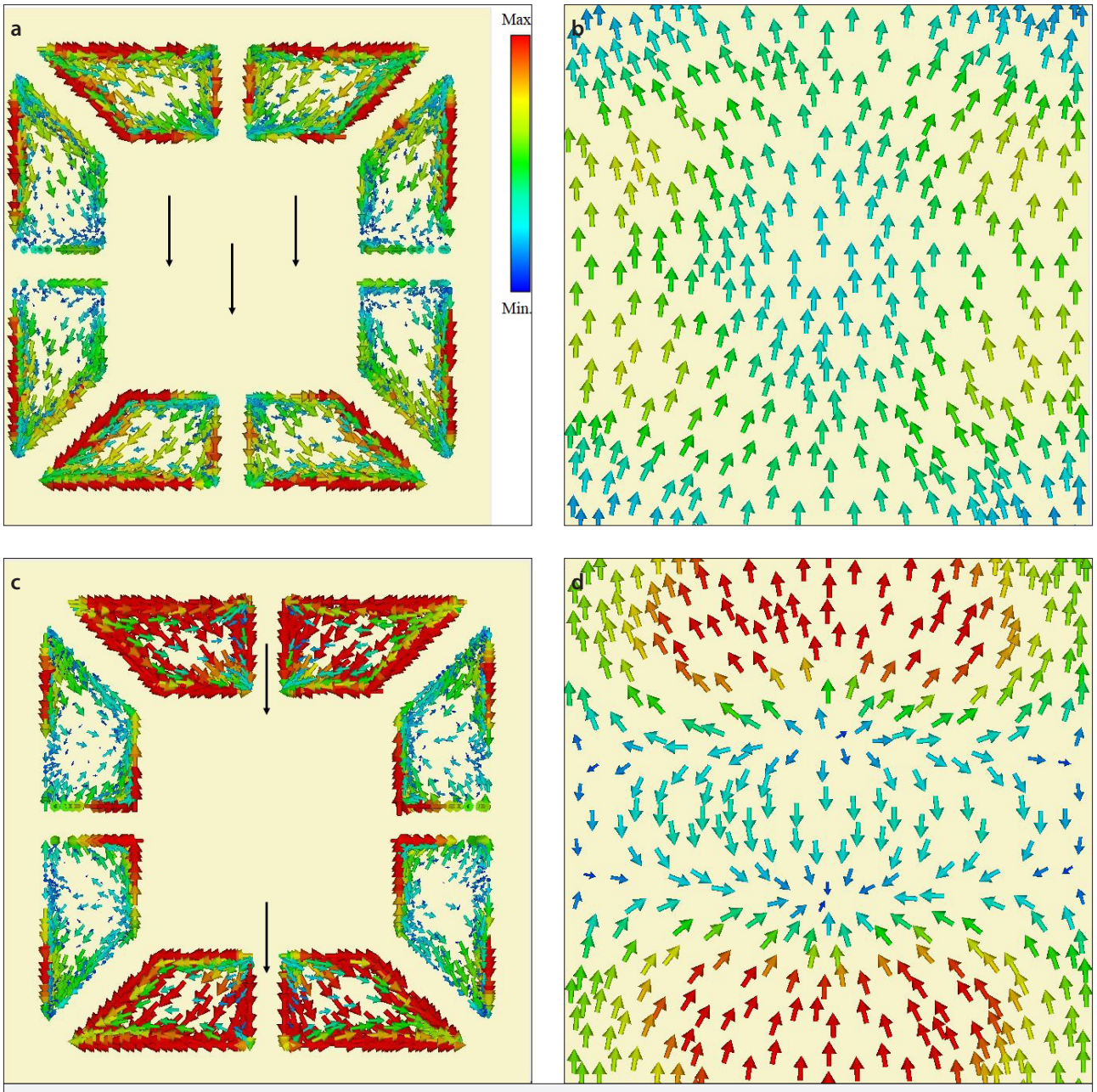

Figure 6. a-d. Vector current distribution at the center frequency of 15 GHz (a) on the top layer (b) on the bottom layer (c) on the top layer (d) on the bottom layer

Results and Discussion

Figure 2a shows the spectral response of the proposed MA under normal incidence for transverse electric (TE) polarization. As shown in the figure, the first unit-cell design with a bare metallic pattern shows two clear resonance peaks around 16.5 and 18 GHz. It is evident that the final optimized unit cell with eight lumped resistors covers the entire K_u-band of 12.4–17.6 GHz with an absorptivity of more than 90%. This outcome proves that the configuration of the lumped resistors in the resonance pattern gives a dramatic rise in the absorptivity over the operation band. Thus, the proposed structure starts to show broadband characteristics. The MA provides an absorption of >90% in the frequency region of 12.4–17.6 GHz, corresponding to a 5.2-GHz, 10-dB bandwidth as shown in Figure 2b. The full-width-at-half-maximum bandwidth of 15.05 GHz is observed ranging from 9.65 to 24.7 GHz. Moreover, the perfect absorption peak is achieved around 15.8 GHz with an absorptivity of ~99.9%. The optimized values of the unit-cell dimensions are as follows: P=13.75 mm, a=3.4 mm, b=5.5 mm, h=1.7 mm, w=1 mm, and R=260 Ω.

Table 1. Comparison of the proposed metamaterial absorber (MA) with previously published MAs

Reference	Thickness (mm)	Unit-Cell Size (mm)	–10 dB Bandwidth	Load-Lumped Element
[12]	3.5 (0.150 λ_0)	15	8.3–17.4	No
[14]	6 (0.217 λ_0)	12.8	6.79–14.96	Yes
[15]	3 (0.109 λ_0)	15.5	9.5–12.4	Yes
[17]	3.2 (0.109 λ_0)	16.6	7.8–12.6	Yes
[19]	3 (0.125 λ_0)	12	7.93–17.18	Yes
[20]	2.6 (0.123 λ_0)	8.4	8–18	No
[21]	10 (0.433 λ_0)	40	8–18	Yes
Proposed MA	1.7 (0.085 λ_0)	13.75	12.4–17.6	Yes

The optimization was first followed to determine the exact dimensions of the metallic pattern. Figures 3a and b show the spectral response depending on *a* and *b*. It is evident that while absorptivity shifts to higher frequencies with an increase in *a*, it moves to lower frequencies with increase in *b*. Figure 3c depicts the spectral response of the proposed MA by varying the thickness of the dielectric substrate from 1.3 to 2.1 mm with a step of 0.2 mm. It is found that when the thickness of the dielectric substrate increases, the absorptivity shifts to a lower frequency band, and thus narrows the bandwidth. The optimized value of dielectric thickness is 1.7 mm, corresponding to $\sim \lambda/14.7$ and $\sim \lambda/10$ at 12 and 18 GHz, respectively. *R* was next to be optimized. Although *R* causes absorptivity, it does not affect resonance frequency according to the RLC circuit model, which is given by

$$f = \frac{1}{2\pi\sqrt{LC}} \tag{5}$$

Bandwidth (*BW*) can be controlled using *R* based on the relationship $BW = f / Q_L$, where Q_L represents the collective loss in the metallic pattern [17]. Figure 3d shows the variations in the absorption spectra with changing *R*. The MA shows similar characteristics as mentioned above within the dynamic range of *R* over 180–340 Ω, and the best response is achieved for *R*=260 Ω. It should be noted that the eight resistors employed in the pattern possess same *R*. Figure 3e illustrates the metamaterial response with *P* from 12.6 to 14.2 mm.

To further understand the MA behavior, the absorption performance was investigated depending on different polarizations and incident angles. The polarization behavior is depicted in Figure 4. The absorption intensity remains stable at different polarization angles, ranging from 0° to 90° for normal wave illumination with both TE and transverse magnetic (TM) modes. It is evident that the MA is polarization insensitive owing to its symmetric geometry. Figure 5 presents the absorption spectra as a function of incidence angle for both the TE and TM polarizations. The incident angle is varied up to 50°. It is observed that broadband absorption is achieved around 80% with an incidence angle of 40° in the frequency band of 12–18 GHz for TE polarization as shown in Figure 5a. For TM polarization, the decrease in absorptivity is clear around 12.5 GHz. However, over the entire K_u-band, absorption remains higher than 80% and 75% at wide incidence angles up to 30° for the TE and TM polarizations, respectively.

To investigate the physical mechanism of the absorption, the vector current distribution and electric-field profile of the proposed MA was analyzed. The simulations were performed at 15 GHz, the center frequency of the K_u-band, and 15.8 GHz, at which near-perfect absorption (~99.9%) was achieved. Figures 6a and b show the vector current distributions on the top and bottom layers under the TE-polarized wave illumination at 15 GHz. It is observed that the currents at the top and bottom layers are out of phase (antiparallel), forming a magnetic dipole opposite to the incident magnetic field. As shown in Figure. 6c and d, two different current vortex points on the bottom layer and the reverse current distribution on the top layer are the origins of the strong magnetic resonance at 15.8 GHz. The antiparallel and vortex current distributions form the magnetic resonance. The electric field is substantially localized in the gaps between the metallic sections at 15 GHz as shown in Figure 7a. At the resonance frequency of 15.8 GHz, the inner and outer sides of the slotted rings are strongly coupled to the incident electric-field vector (Figure 7b). Furthermore, the electric-field coupling from the gaps leads to the high electromagnetic energy absorption of the incident wave across the terminals of the lumped resistors. This absorption mechanism is active up to 18 GHz, which is the origin of the broadband absorption characteristics of the MA.

The dispersive input impedance of the MA was further analyzed to gain insights into its broadband characteristics. As shown in Figure 8, where the real part of Z_{in} is close to 1, the imaginary part of Z_{in} is near zero over the operation band. These outcomes prove that the impedance matching condition is satisfied, leading to near-zero reflection from the metamaterial.

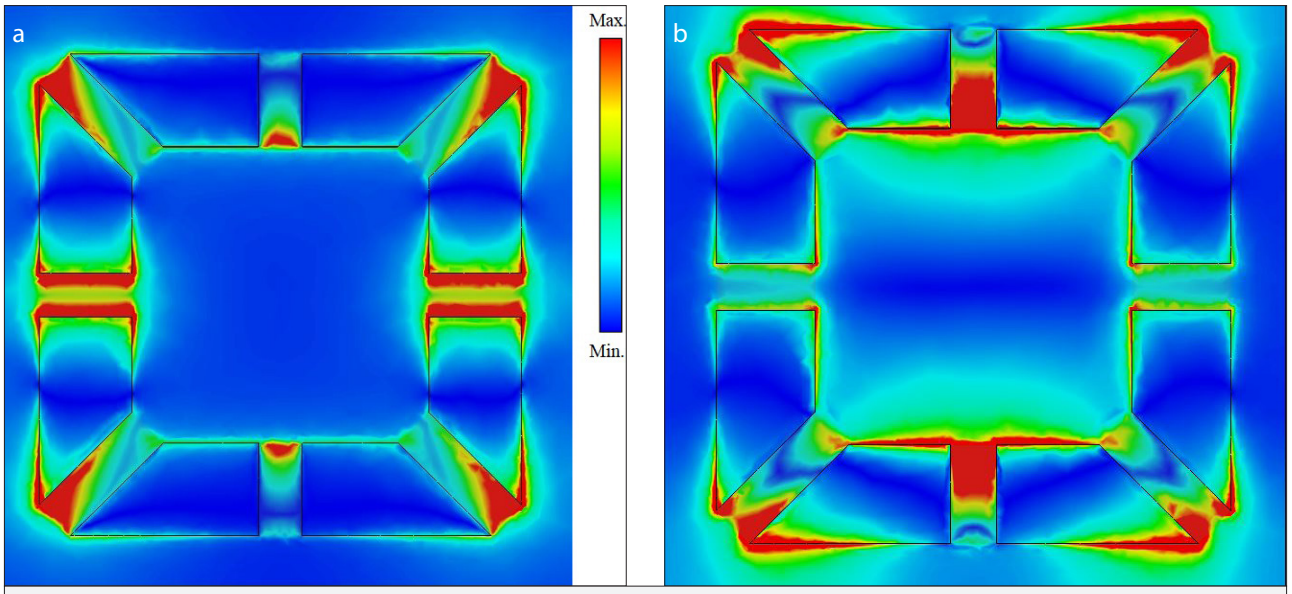

Figure 7. a, b. Electric field profile at 15.8 GHz (a) on the top layer (b) on the bottom layer

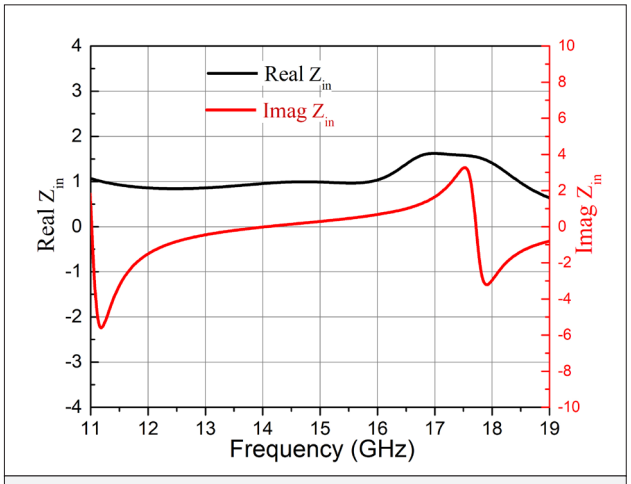

Figure 8. Simulated input impedance of Zin of the proposed MA

Finally, the proposed MA is compared with previously reported designs. Table 1 presents the absorber characteristics in terms of the dielectric thickness, unit-cell size, –10-dB bandwidth, and use of a lumped element. It can be observed that the proposed MA is very thin at 1.7 mm, corresponding to 0.085 λ_0 in terms of free-space wavelength at the center frequency of the K_u-band, and compact compared with other designs. Therefore, the proposed MA is very suitable for practical broadband applications in the K_u-band, in which a thin absorbent layer coating is required.

Conclusions

In this study, a broadband MA was numerically investigated. The broadband characteristics of the MA were verified using electric field, current density, and the input impedance profiles. Owing to its structural symmetry, the proposed MA has a polarization insensitive response over the entire K_u-band. Wide incidence-angle absorption is achieved up to 30° for the TE and TM polarizations with the absorption ratios higher than 80% and 75% in the frequency range of 12–18 GHz, respectively. Furthermore the proposed MA is very thin at 0.085λ_0 mm. These results show that the proposed MA is a promising candidate for use in K_u-band spectral imaging, radar stealth, and thermal radiometers.

Peer-review: Externally peer-reviewed.

Conflict of Interest: The author has no conflicts of interest to declare.

Financial Disclosure: The author declared that the study has received no financial support.

References

1. N. Garcia, M. Nieto-Vesperinas, "Left-Handed Materials Do Not Make a Perfect Lens". Phys. Rev. Lett., vol. 88, no. 20, pp. 207403-4, May, 2002. [Crossref]
2. M. M. Hasan, M. R. I Faruque, M. T. Islam, "Dual band metamaterial antenna for LTE/bluetooth/WiMAX system", Sci. Rep., vol. 8, no. 1240, pp. 1-17, Jan. 2018. [Crossref]
3. Y. Xie, X. Fan, Y. Chen, J. D. Wilson, R. N. Simons, J. Q. Xiao, "A subwavelength resolution microwave/6.3 GHz camera based on a metamaterial absorber", Sci. Rep., vol. 7, no. 40490, pp. 1-8, Jan. 2017. [Crossref]
4. D. R. Smith, Willie J. Padilla, D. C. Vier, S. C. Nemat-Nasser, S. Schultz, "Composite Medium with Simultaneously Negative Permeability and Permittivity", Phys. Rev. Lett., vol. 84, pp. 4184-4187, May, 2000. [Crossref]
5. D. R. Smith, S. Schultz, P. Markoš, M. Soukoulis, "Determination of effective permittivity and permeability of metamaterials from reflection and transmission coefficients", Phys. Rev. B - Condens. Matter Mater. Phys., vol. 65, no. 19, pp. 195104-5, Apr. 2002. [Crossref]

6. J. B. Pendry, D. Schurig, D. R. Smith, "Controlling electromagnetic fields", Science, vol. 312, no. 5781, pp. 1780-1782, June, 2006. [Crossref]
7. G. T. Ruck GT, D. E. Barrick DE, W. D. Stuart WD, C. K. Krichbaum, "Radar Cross Section Handbook", Springer US, New York, USA, 1970. [Crossref]
8. W. W. Salisbury, "Absorbant body for electromagnetic waves", US Pat., no. 486608, June, 1952.
9. D. R. Smith, J. B. Pendry, M. C. K. Wiltshire, "Metamaterials and negative refractive index", Science, vol. 305, no. 5685, pp. 788-792, Aug. 2004. [Crossref]
10. P. Yu et al., "Broadband Metamaterial Absorbers", Adv. Opt. Mater., vol. 7, no. 3, pp. 1800995-32, Feb. 2019.
11. S. Gu, B. Su, X. Zhao, "Planar isotropic broadband metamaterial absorber", J. Appl. Phys., vol. 114, no. 16, pp. 163702-6, Oct. 2013. [Crossref]
12. C. Zhanga, Q. Chenga, J. Yang, J. Zhao, T. J. Cui, "Broadband metamaterial for optical transparency and microwave absorption", Appl. Phys. Lett., vol. 110, no. 14, Apr. 2017. [Crossref]
13. Y. J. Yoo et al., "Metamaterial absorber for electromagnetic waves in periodic water droplets", Sci. Rep., vol. 5 pp. 14018-8, Sep. 2015. [Crossref]
14. M. Yoo, S. Lim, "Polarization-independent and ultrawideband metamaterial absorber using a hexagonal artificial impedance surface and a resistor-capacitor layer", IEEE Trans. Antennas Propag., vol. 62, no. 5, pp. 2652-2668, May, 2014. [Crossref]
15. T. T. Nguyen, S. Lim, "Design of Metamaterial Absorber using Eight-Resistive-Arm Cell for Simultaneous Broadband and Wide-Incidence-Angle Absorption", Sci. Rep., vol. 8, no. 6633, pp. 2075-10, Apr. 2018. [Crossref]
16. M. S. Islam, Md. Samsuzzaman, G. K. Beng, N. Misran, M. T. Islam, "A Gap Coupled Hexagonal Split Ring Resonator Based Metamaterial for S-Band and X-Band Microwave Applications", IEEE Access, vol. 8, pp. 68239-68253, Apr. 2020. [Crossref]
17. T. Q. H. Nguyen, T. K. H. Nguyen, T. N. Cao, H. Nguyen, L. G. Bach, "Numerical study of a broadband metamaterial absorber using a single split circle ring and lumped resistors for X-band applications", AIP Adv., vol. 10, no. 3, pp. 035326-1, Mar. 2020. [Crossref]
18. CST Microwave Studio, http://www.cst.com, CST GmbH, Darmstadt, Germany.
19. S. Li, J. Gaoa, X. Cao, W. Li, Z. Zhang, D. Zhang, "Wideband, thin, and polarization-insensitive perfect absorber based the double octagonal rings metamaterials and lumped resistances", J. Appl. Phys., vol. 116, no. 4, pp. 043710-6, July, 2014. [Crossref]
20. L. Sun et al., "A simplified design of broadband metamaterial absorber covering X- And Ku- band", Mater. Res. Express., vol. 6, no. 12, pp. 125805-112, 2019. [Crossref]
21. J. Yang, Z. Shen, "A thin and broadband absorber using double-square loops", IEEE Antennas Wirel. Propag. Lett., vol. 6, pp. 288-291, Oct. 2007. [Crossref]

Sinan Aksimsek received his B.Sc. degree in Electrical and Electronics Engineering, and his M.Sc. degree in Electronics and Telecommunication Engineering from Istanbul University and Istanbul Technical University, Istanbul, Turkey, in 2007 and 2010, respectively. He received his Ph.D. degree in Electronics Engineering from the Gebze Technical University, Kocaeli, Turkey, in 2014. From 2015 to 2016, he was a postdoctoral research fellow with the Department of Electronics and Nanoengineering, Aalto University, Finland. He is currently the Assistant Professor with the Department of Electrical and Electronics Engineering, İstanbul Kultur University, İstanbul, Turkey. His current research interests include mm-wave antenna technologies, metasurfaces and metamaterials, printed and flexible RF devices, electromagnetics of 2D materials, and graphene plasmonics.